Anal. Bioanal. Electrochem., Vol. 8, No. 3, 2016, 382-396

Analytical & Bioanalytical Electrochemistry

2016 by CEE
www.abechem.com

Full Paper

Surface-modified Electrodes: Oxidative Electropolymerisation of Macrocyclic Complexes of Fe(III) and Ni(II)

Anuj Kumar* and Randhir Singh

Research Scholar, Department of Chemistry Gurukula Kangri University Haridwar-249404, India

*Corresponding Author, Tel.: +919761565732

E-Mail: anujkumar9791@gmail.com

Received: 15 February 2016 / Received in revised form: 2 May 2016 / Accepted: 3 May 2016 / Published online: 15 May 2016

Abstract- Me_2-dibenzo[b,k]-dipyridyl[f,o][1,4,7,10,13,16]-hexaaza-5,9,14,19-tetraoxo-cyclooctadecane macrocyclic complexes of Fe(III) and Ni(II) have been synthesized by template method and analysed with various techniques like molar conductance, FT-IR, UV-Vis, Mass spectra. The studies of surface-modified electrode based on tThe oxidative electropolymerisation of the monomeric Fe[Me_2-(DBDPy)N_6tetraoxo[18]Cl_2]Cl and Ni[Me_2-(DBDPy)N_6tetraoxo[18]Cl_2] complexes were carried out on the Pt electrode in DMSO containing 0.1 M TEAP, by employing cyclic voltammetry. A thin film of polymer, [M-Me_2-(DBDPy)N_6tetraoxo[18]Cl_2]n , where M=Fe(III) and Ni(II), was formed on the electrode surface by constant potential electrolysis at 1.5 V on cycling from -1.5 to +2.0 V *vs* Ag/AgCl.The monomers, after polymerization form [M-Me_2-(DBDPy)N_6tetraoxo[18]Cl_2]n , where M=Fe(III) and Ni(II), which form a thin film on the electrode surface. The film formed on the electrode surface by constant potential electrolysis at 1.5 V on cycling from -1.5 to +2.0 V *vs* Ag/AgCl The magnitude of film growth depends on the method of deposition in the solvent and the rate of cycling i.e 10 cycles from -1.5 to +2.0 V *vs* Ag/AgCl at 200 mVs^{-1} scan rate resulted in “Polymer layers” formation on Pt electrode. Film growth was also dependent on the concentration of the electrolyte and the electrode surface and found that the heterogeneous electron transfer rate constant is increased with the growth of the film. UV-Visible and FT-IR spectra suggest that the macrocycles remained in the polymeric film.

Keywords - Macrocycles, Electropolymerisation, Polymeric film, Surface modified electrode

1. INTRODUCTION

The polymeric film coated surface modified electrodes have been claimed as a mean of obtaining many electrochemical advantages. Special attention focused on the modification of electrode surfaces with macrocyclic complex polymeric films. Electrochemical polymerisation has paved the way for immobilization of the tetraazamacrocyclic complexes on the electrode surface. Polymerization is based on the electrochemical redox process of monomers to form a polymeric film incorporating the macrocyclic complexes. A thin film of poly-Ni(II) tetraazaannulene showed the oxidation of carbohydrate, methanol and water systems [1-3]. The voltammetric behaviour of the polymeric films formed of Ni(II) planar macrocyclic complex is not yet fully understood. Two postulates have been put forward; one consider that upon the electrochemical polymerization of Ni(II) complex in alkaline media, the nickel and tetraaza environment of the macrocyclic complex incorporated in the polymeric film, behave in a similar manner as nickel hydroxide electrode. The second postulate reveals that the complex does not decompose upon electropolymerisation but attached to the electrode surface and remains therein *via* oxo-bridges [4-9]. Understanding electron propagation or charge transport in polymeric film of electroactive species began with electron hopping between adjacent, localized redox sites and polymeric film peak currents were found out. Charge transport rates in the terms of electron diffusion coefficients (D_E or D_{ct}) have been determined and theoretical analysis of electron diffusion and a sequence of electron self-exchange reaction during polymerisation has been proposed [10-15].

The polymeric films are intriguing due to several viewpoints such as these may mimic the catalytic redox behaviour of biological systems. The formation of polymeric film of macrocyclic complexes onto the electrode surface enhanced the electrochemical response to numerous important analytes and has shown good mechanical and chemical stability with high degree of compatibility towards both aqueous and nonaqueous solvents. Generally, at electrode surface, immobilized polymeric films formed of monomeric macrocyclic complexes containing redox couples act as electron transfer media for another electroactive species which show redox behaviour [16-20].

Applications of modified electrode surface in mediated oxidation-reduction of electroactive species solution by immobilized redox-catalyst reagents, by bonded or absorbed monolayer or by ion exchange polymer coatings are known [21]. Electropolymerized polymeric films have potentially greater stability and chemical diversity, but offer electrocatalytic kinetics of electroactive species with many possible rate controlling steps [22-24]. Recent applications of metal-functionalized polymers obtained via electropolymerisation are promising. Surface modified electrodes are found to facilitate carbon dioxide reduction. Recently modified electrode has been reported as sensor for detection of enzymes like glycosidases which cleave gycosidic bond in carbohydrates [25].

In this communication, the polymeric films of Me_2-dibenzo[b,k]-dipyridyl[f,o][1,4,7,10,13,16]-hexaaza-5,9,14,19-tetraoxo-cyclooctadecane macrocyclic complexes of Fe(III) and Ni(II) {Fe[Me_2-(DBDPy)N_6tetraoxo[18]Cl_2]Cl and Ni[Me_2-(DBDPy)N_6tetraoxo[18]Cl_2} have been prepared with the help of electropolymerisation by employing cyclic voltammetry and taken into account for studies.

2. EXPERIMANTAL

2.1. Chemicals, equipment, methods and materials

All the chemicals (of AR grade) such as 2,4-diaminotoleune, diethyl-2,6-pyridinecarboxylate, ferric chloride, hydrated nickel chloride, DMSO, methanol and acetone (of AR grade) were purchased from TCI India and used without further purification. The elemental analysis (C, H, N) and mass spectral studies of the macrocyclic complexes were carried out at central instrumental laboratory, Punjab University Chandigarh, India (Eager Xperience and TOF MS ES+6018e3). Infrared spectra were recorded on a FT-IR 8400S (Shimadzu, Kyoto, Japan) using KBr pallets. The electronic spectra were recorded on Double Beam 2550 UV-Vis Spectrophotometer (Perkin Elmer CT, USA) using DMSO as solvent. The molar conductance was recorded on Auto Ranging Conductivity/TDS Meter (TCM 15+). Electrochemical measurements were carried out using Metrohm 663 VA Stand auto lab instrument (Metrohm AG, Netherlands) using three electrode system consists of Pt disc electrode (0.031 cm^2) as a working electrode, Ag/AgCl (3 M KCl) reference electrode and Pt wire electrode as auxiliary electrode. Pre-treatment of electrodes was done before every cyclic voltammetric experiments.

2.2. Preparation of the Macrocyclic complexes

The macrocyclic complexes were synthesized according to literature method [26]. The detailed procedure is as follow:

2.2.1. Synthesis of Fe[Me_2-(DBDPy)N_6tetraoxo[18]Cl_2]Cl

2,4-diaminotoluene (0.244 g, 2 mole), diethyl-2,6-pyridiniumcarboxylate (0.446 g, 2 mole) and iron (III) chloride (0.162 g, 1 mole) were dissolved in 50 mL methanol in round bottom flask. The reaction mixture was refluxed for 6-8 hours. A dark brown coloured reaction mixture was obtained, which then concentrated and the concentrate was kept in desiccator overnight. Dark brown coloured crystals of macrocyclic complex appeared, which was then filtered, and washed with methanol, acetone and diethyl ether and dried in vacuum. The crystals were recrystallized, and characterized by spectroscopic techniques like CHN, UV-Vis, FT-IR, and mass spectra. Analytical data are as given below and scheme for the synthesis of (a) Fe[Me_2-(DBDPy)N_6tetraoxo[18]Cl_2]Cl is shown in Fig. 1.

Yield: 0.19 g (75%), Mp: 210 °C; Mol. Condc. ($Ohm^{-1}cm^2mol^{-1}$): 47; Anal. Calc. for $Fe[C_{28}H_{22}N_6O_4\ Cl_2]Cl$: C, 50.37; H, 03.29; N, 12.59. Found: C, 50.64; H, 3.57; N, 11.13%; MS (fragments are based on ^{56}Fe and ^{35}Cl): m/z 597.23 $(MH)^+$ (Calc. 597.14); FTIR (ν_{max}/cm^{-1}): 3295 (N-H), 1670 (C=O), 1451 (C-N), 1120 (C-CH_3), 535 (Fe-N) cm^{-1}. UV-Vis: 18281 cm^{-1} ($^5T_{2g} \rightarrow {}^5E_g$); L. F. parameters: D_q (1132 cm^{-1}), B' (955 cm^{-1}), β (0.83); Stereochemistry: Octahedral.

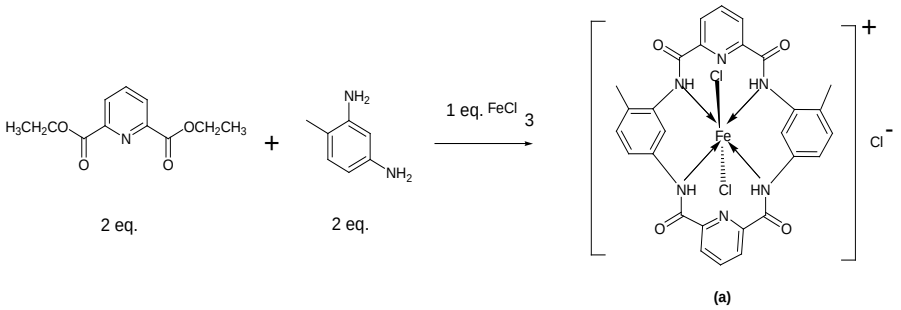

Fig. 1. Scheme for the synthesis of Fe(III) macrocyclic complex, Fe[Me_2-(DBDPy)N_6tetraoxo[18]Cl_2]Cl (a)

2.2.2. *Synthesis of Ni[Me_2-(DBDPy)N_6tetraoxo[18]Cl_2]*

2,4-diaminotoluene (0.244 g, 2 mole), diethyl-2,6-pyridiniumcarboxylate (0.446 g, 2 mole) and nickel (II) chloride hexahydrate (0.198 g, 1 mole) were dissolved in 50 mL methanol in round bottom flask. Rest of the method was similar as described above. Analytical data are as given below and scheme for the synthesis of (b) Ni[Me_2-(DBDPy)N_6 tetraoxo[18]Cl_2 is shown in Fig. 2.

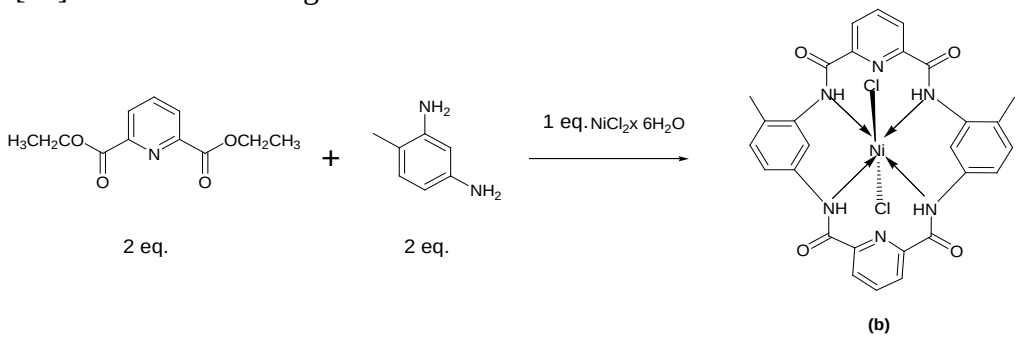

Fig. 2. Scheme for the synthesis of macrocyclic complex, Ni[Me_2-(DBDPy)N_6tetraoxo[18]Cl_2] (b)

Yield: 0.23 g (85%), Mp: 225 °C; Mol. Condc. ($Ohm^{-1}cm^2mol^{-1}$): 45; Anal. Calc. for $Ni[C_{28}H_{22}N_6O_4]Cl_2$: C, 52.83; H, 03.46; N, 13.21. Found: C, 53.23; H, 4.12; N, 12.73%; MS (fragments are based on ^{59}Ni and ^{35}Cl): m/z 565.15 $(MH)^+$ (Calc. 565.79); FTIR (ν_{max}/cm^{-1}): 3235 (N-H), 1685 (C=O), 1565 (C-N), 1209 (C-CH_3), 495 (Fe-N) cm^{-1};UV-Vis: 17513 cm^{-1}($^3A_{2g}$ (F)→$^3T_{2g}$(F)), 24875 cm^{-1} ($^3A_{2g}$ (F)→ $^3T_{1g}$(F)), 25512 cm^{-1}($^3A_{2g}$ (F)→ $^3T_{1g}$ (P)); L. F. parameters: D_q (1084 cm^{-1}), 1.4 ($\nu_3/\ \nu_1$), B' (1120 cm^{-1}), β (0.68); Stereochemistry: Octahedral.

3. RESULTS AND DISCUSSION

3.1. Electrochemical studies

Electrochemical behaviour of the macrocyclic complexes were studied by employing cyclic voltammetry. The cyclic voltammograms (CVs) of these complexes (Fig. 3) show quasirreversible redox processes. The observed values for E_{pa} and E_{pc} for both macrocyclic complexes are comparable to analogous macrocyclic complexes reported earlier (Table 1).

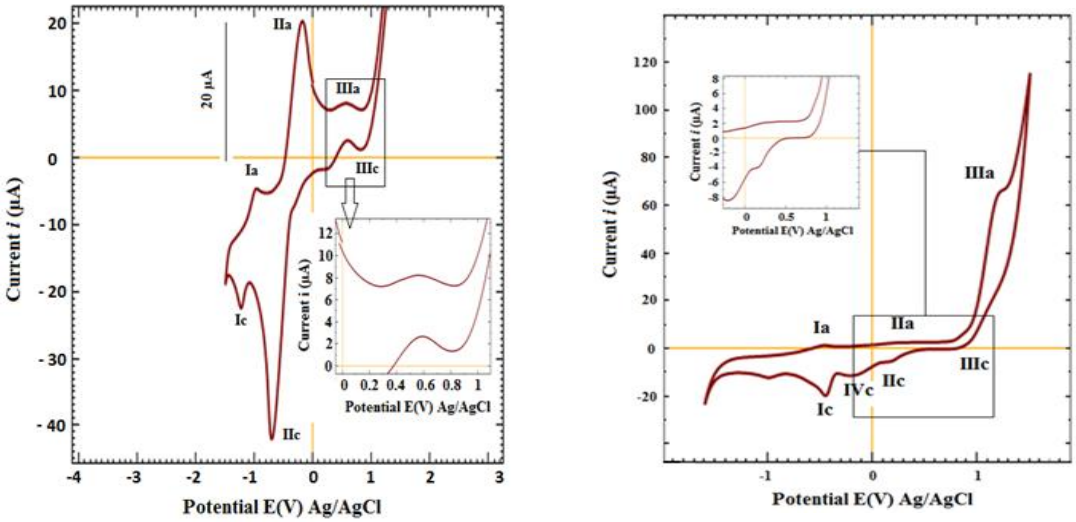

(a) **(b)**

Fig. 3. CV of **(a)** Fe[Me_2-(DBDPy)N_6tetraoxo[18]Cl_2]Cl and **(b)** CV of Ni[Me_2-(DBDPy)N_6tetraoxo[18]Cl_2], recorded in DMSO (1×10^{-3} M) containing 0.1 M TEAP solution as supporting electrolyte at a scan rate of 100 mVs^{-1}. The inserts are enlarged portions of the CVs indicated by the arrows.

On single scanning at 200 mVs^{-1}, the typical CV (Fig. 3a) of Fe[Me_2-(DBDPy)N_6tetraoxo[18]Cl_2]Cl complex in DMSO solution containing 0.1 M TEAP. In the forward scan, the voltammogram of this complex showed three anodic peaks (Ia, IIa and IIIa) appear at -1.0 V, -0.20 V and +0.60 V respectively while on reverse scanning three cathodic peaks (Ic, IIc and IIIc) are observed at -1.2 V, -0.70 V and +0.80 V. The corresponding redox couples are assigned to for L/L^{-1} (Ia/Ic), Fe^{3+}/Fe^{2+} (IIa/IIc) and Fe^{2+}/Fe^{+} (IIIa/IIIc) with the formal potentials at -1.10 V, -0.45 V and +0.70 V. All the electrochemical results were observed as quasirreversible redox couples as indicate by their peak separation (ΔE) and peak current ratio (i_{pa}/i_{pc}).

$Fe^{3+}+e^{-}\rightarrow FeL^{2+}$

$FeL^{2+}+e^{-}\rightarrow FeL^{+}$

Peak currents were found stable over repeated scans. The CVs of both macrocycles were also recorded varying scan rates from 50-200 mVs^{-1}. The anodic and cathodic peak potentials were found independent of scan rate for each complex (Fig. 4a and Fig. 5a).

The plots of peak currents (Fig. 4b and Fig. 5b) against the square root of scan rates were found to be linear, following the Randles-Sevcik equation for reversible electrochemical reactions.

$$i=2.69\times10^5\, n^{3/2}AD^{1/2}cv^{1/2} \quad (1)$$

where n is the number of electrons transferred, A is the area of electrode, D is the diffusion coefficient, c is the analyte concentration and v is the scan rate.

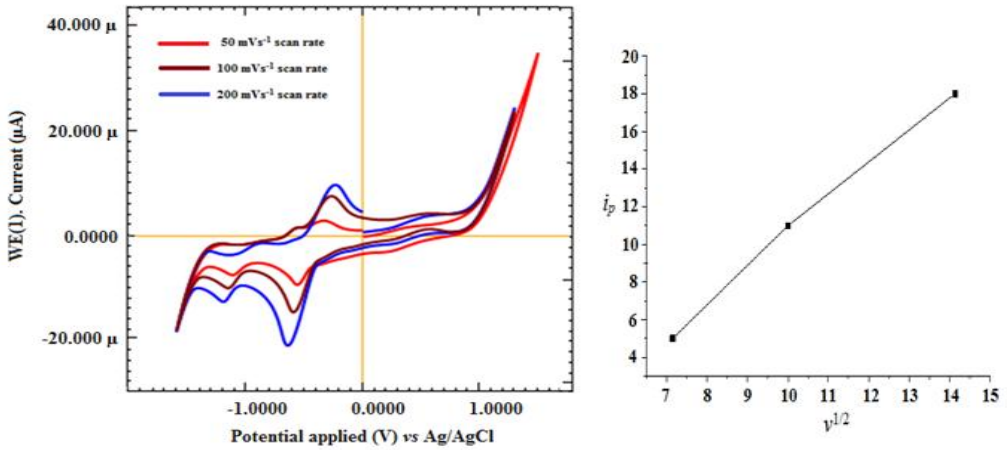

(a) **(b)**

Fig. 4. (a) CV of Fe[Me_2-(DBDPy)N_6tetraoxo[18]Cl_2]Cl at different scan rates (50-200 m Vs^{-1}) and; **(b)** Plot of i_p *vs* $v^{1/2}$ for Fe[Me2-(DBDPy)N6tetraoxo[18]Cl_2]Cl

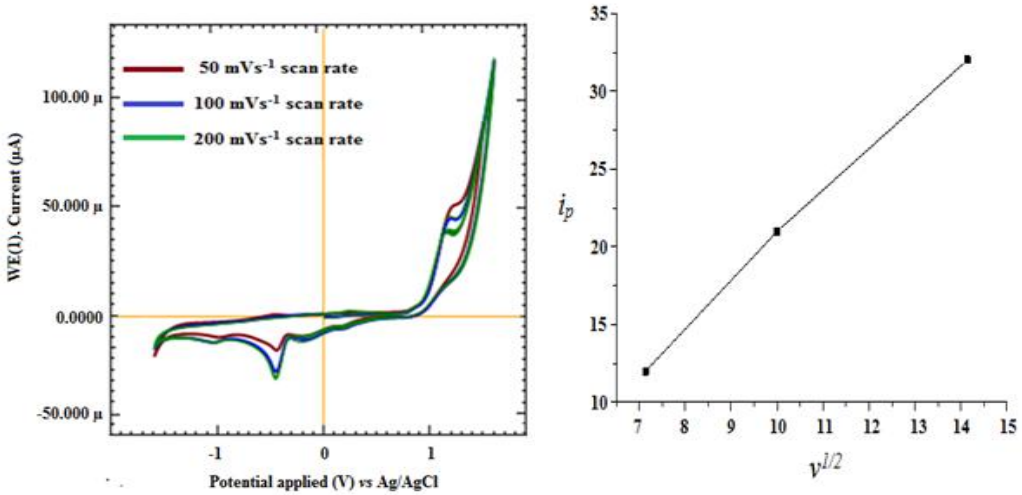

(a) **(b)**

Fig. 5. (a) CV of Ni[Me2-(DBDPy)N6tetraoxo[18]Cl_2] at different scan rates (50-200 m Vs^{-1}) and **(b)** Plot of i_p *vs* $v^{1/2}$ for Ni[Me2-(DBDPy)N6tetraoxo[18]Cl_2]

3.2. Polymeric film modified electrode

In this communication, electropolymerisation of Fe[Me2-(DBDPy)N6tetraoxo[18]Cl_2] Cl and Ni[Me_2-(DBDPy)N6tetraoxo[18]Cl_2] monomers have been carried out onto Pt disc electrode by employing cyclic voltammetric technique in the nitrogen atmosphere. The polymeric film deposition of both macrocyclic complexes take place on the continuous cycling of the electrode potential range between -1.5 and +2.0 V *vs* Ag/AgCl employing 10 cycles at scan rate 100-200 mVs^{-1}. The kinetic aspects viz. diffusion coefficient, heterogeneous electron transfer rate constant and charge profile also have been taken into account.

CVs of (a) Fe[Me_2-(DBDPy)N_6tetraoxo[18]Cl_2]Cl and (b) Ni[Me2-(DBDPy)N6tetraoxo[18]Cl_2] macrocyclic complexes, as obtained during the continuous cycling in the DMSO solution containing 0.1 M TEAP are shown in Fig. 6. For both the macrocycles, the formation and growth of a polymeric film on the Pt electrode surface was observed with the increase in size of the redox peaks and it showed the continuous interaction of the macrocycles onto the Pt electrode forming polymeric films. The redox couples Fe^{3+}/Fe^{2+}, Fe^{2+}/Fe^{+} and Ni^{2+}/Ni^{3+}, Ni^{2+}/Ni, which are the main electrochemical quasirreversible redox processes, are also observed in CVs with repeated scan. The peak current intensity is proportional to the potential sweep rate over a wide range (50-200 mVs^{-1}), as expected for an electroactive species deposited on the surface of an electrode.

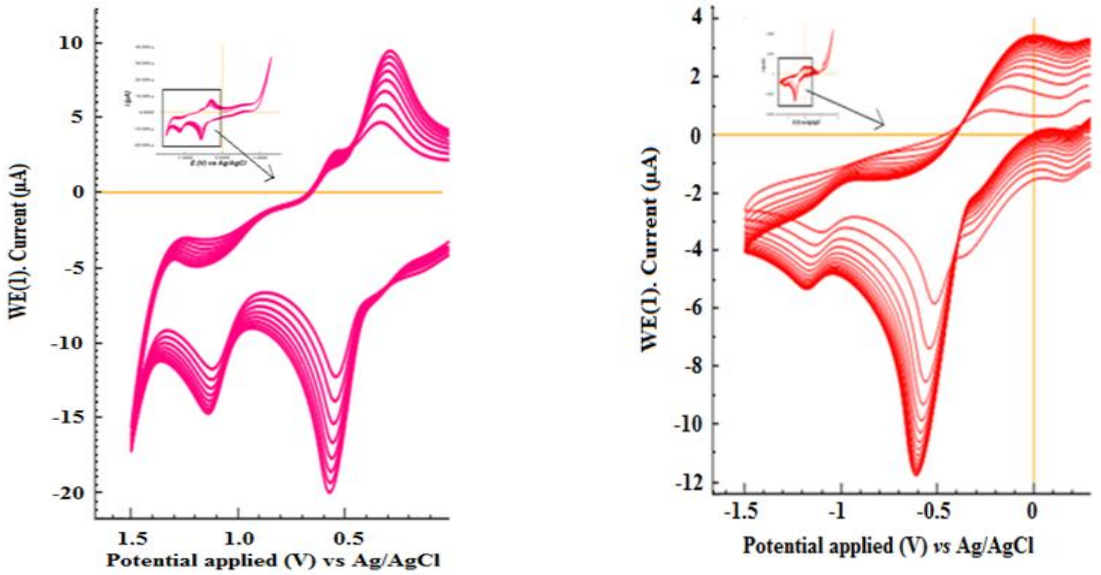

(a) **(b)**

Fig. 6. Repeated scan CV of **(a)** Fe[Me2-(DBDPy)N6-tetraoxo[18]Cl_2]Cl and **(b)** CV of Ni[Me2-(DBDPy)N6-tetraoxo[18]Cl_2] showing electropolymerisation, recorded in DMSO (1×10^{-3} M) containing 0.1 M TEAP solution as supporting electrolyte at 100 mVs^{-1} scan rate. The inserts are enlarged portions of the CVs indicated by the arrows.

The CVs for both macrocyclic complexes showed the oxidation peaks shifting in an anodic direction and the reduction peaks shifting in the cathodic direction with the increase in current for both the peaks. This electrochemical behaviour represents the conductive nature of formed polymeric films. The film deposited on the Pt electrode are distinctly visible and on dissolving the film in chloroform, light yellow and light green colour were observed for Fe[Me_2-(DBDPy)N_6tetraoxo[18]Cl_2]Cl and Ni[Me2-(DBDPy)N6tetraoxo[18]Cl_2] complexes respectively. It is noteworthy that the redox couple Fe^{2+}/Fe^{3+} and Ni^{3+}/Ni^{2+} involve a metal-localized redox process. The electrochemical deposition is controlled by the electrode potential. Generally the growth of polymeric films on the electrode surface controlled the amount of deposited material. This phenomenon can be easily attained by monitoring the total charge passed during the electropolymerisation. When electropolymerisation phenomenon take place at the electrode surface, the electroactive species come into actual physical contact of the electrode surface so there is a potential gradient around the electrode and ions of diffusing molecules will reach a point at which the potential is sufficiently bring the polymerisation at the electrode surface. In electropolymerisation, electroactive monomers have been coupled directly onto the electrode surface via radical producing reaction. The polymeric film formation is affected by the technique of the electrochemical oxidation. Consequently, for both macrocycles, two redox processes E_{p1} and E_{p2} are prime steps in the mechanism of removal of electron at E_{p1} may be resulted in the formation of π cation radicals, which may coupled as dimers as an "intermediate". The redox processes were observed near -0.65 V to +0.25 V at scan rate >100 mVs^{-1}. Removal of electrons at E_{p2} resulted in the formation of π dication diradicals which swiftly coupled to form a polymer and deposited on the electrode surface as polymeric film.

3.3. Characterisation of the polymeric modified electrode

Constant-potential electrolysis at 1.5 V *vs* Ag/AgCl yielded polymeric film on the Pt electrode followed by dissolution in DMSO. The lowest energy transition of the monomers at 547 nm for macrocyclic complex (a) and 571 nm for macrocyclic complex (b) is shifted to 629 nm and 635 nm respectively on polymeric film formation. The red shift in the UV-Vis spectra of polymeric films can be explained by the degree of π electron delocalization in the macrocyclic framework. The π electron delocalization is enhanced in polymeric film due to increase in conjugation resulting in red shift (Fig. 7 and Fig. 8).

The FT-IR spectra of solid deposited polymeric films showed four bands out of which one band at 3235-3355 cm^{-1} assigned to N-H stretching. Strong peaks at 1195-1372 cm^{-1} indicate C-CH_3 stretching, a C-N stretching at approximately 1450-1485 cm^{-1} and weak band is also appeared at 1669-1695 cm^{-1} which assigned to C=O stretching for both macrocycles. The FT-IR spectra were approximately similar for both monomers to their respective polymers suggesting that the functional groups in ligands remained intact during polymeric

film formation. The sufficient film growth was not observed in the positive potential region, while low film growth occurred when scanning was performed within the potential range (+1.8 V to -0.8 V). However, scanning is extended through the second redox couple for rapid film growth associated with polymer formation.

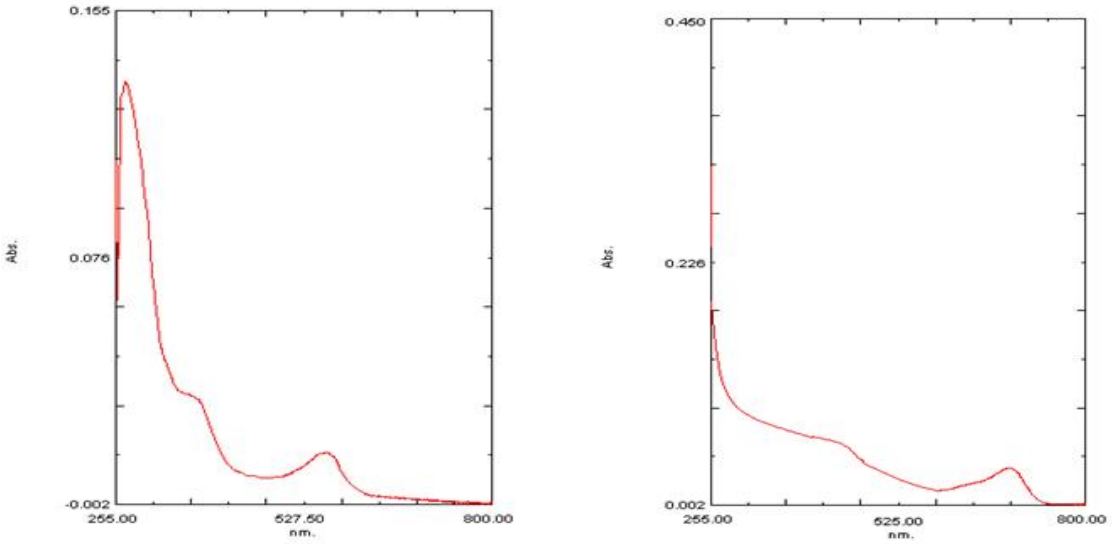

(a) **(b)**

Fig. 7. (a) UV-Vis spectra of Fe[Me_2-(DBDPy)N_6tetraoxo[18]Cl_2]Cl as monomer and **(b)** UV-Vis spectra of Fe[Me_2-(DBDPy)N_6tetraoxo[18]Cl_2]$_n$Cl as polymer

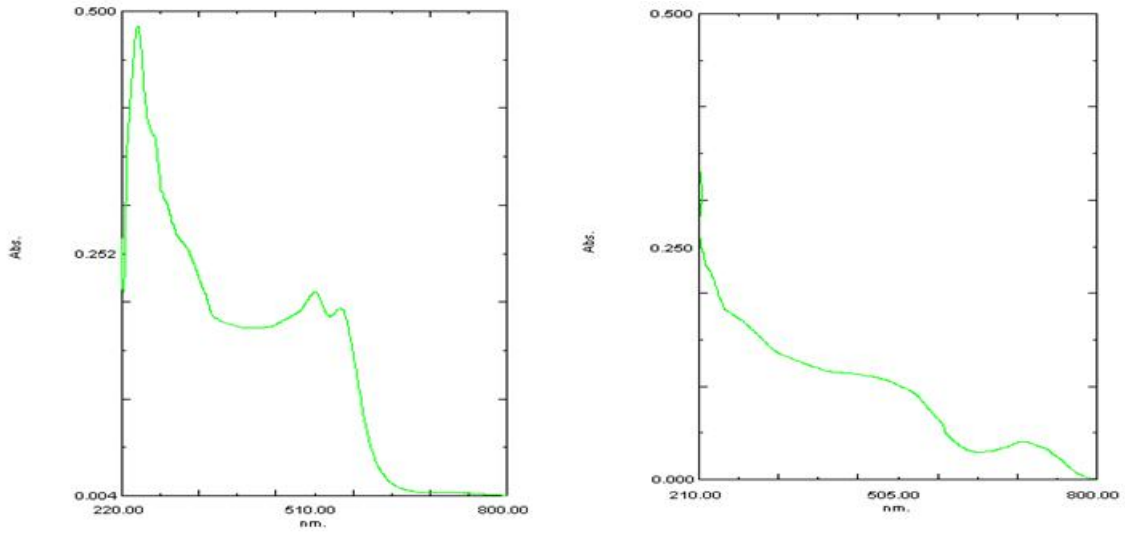

(a) **(b)**

Fig. 8. (a) UV-Vis spectra of Ni[Me_2-(DBDPy)N6tetraoxo[18]Cl_2] as monomer and **(b)** UV-Vis spectra of Ni[Me_2-(DBDPy)N6tetraoxo[18]Cl_2]$_n$ as polymer

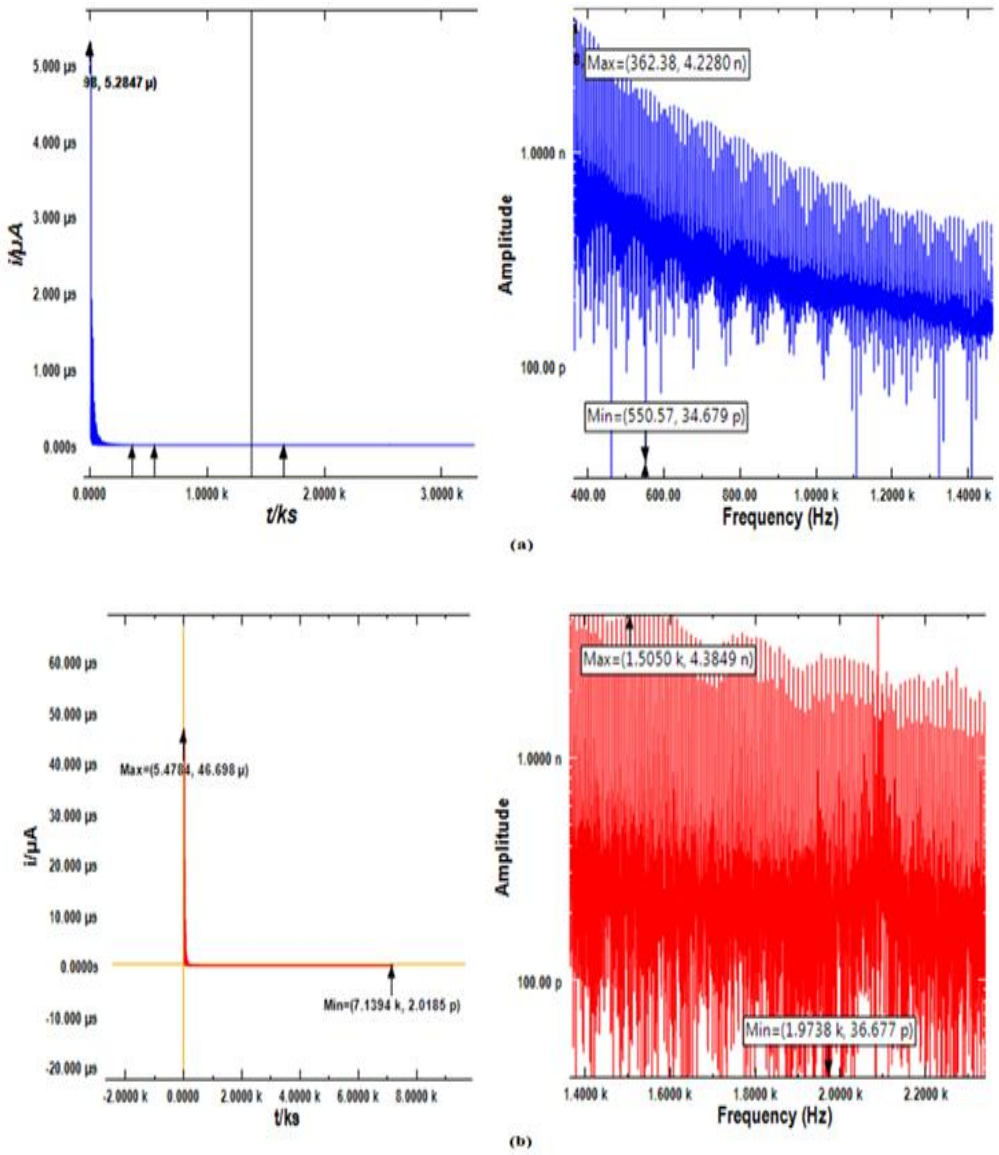

Fig. 9. (a) i *vs* t, Plot of Fe[Me_2-(DBDPy)N_6tetraoxo[18]Cl_2]Cl and **(b)** i *vs* t, Plot of Ni[Me_2-(DBDPy)N_6tetraoxo[18]Cl_2]

3.4. Charge profile

The charge profile, plot i *vs* t (Fig. 9) for both macrocycles do not show a significant growth in the polymeric film over 450 seconds at 200 mVs^{-1}. The voltammetric response indicates that the formed polymeric films of these macrocycles gain stability on the Pt electrode surface immediately. The stability of formed polymeric film is affected by its kinetics parameters like peak separation (ΔE) and i_p and is promoted by scan rate. Peaks symmetry in the oxidation and reduction peaks (Fe^{3+}/Fe^{2+}) (redox couple seemed as mirror image to each other) showed fast propagation of redox state through many monolayers of macrocyclic monomers was compared to the voltammetric time scale which indicates the stability of formed polymeric films.

3.5. Electrochemical Impedance Spectroscopy

Electrochemical impedance spectroscopy (EIS) is used to determine the polymeric film resistance (RF) for these polymeric films. This technique is based on the perturbation of a system at equilibrium by a small amplitude AC potential wave form .

The impedance spectrum (Nyquist plot) for of Ni[Me_2-(DBDPy)N_6tetraoxo[18]Cl_2] (Imonomer) and its polymeric film (IIpolymer) showed in Fig. 10., Nyquist plot (I) for monomer showed a semi-circle curve at high frequencies while it showed a little band line in upward direction at low frequencies. To understand this system, a Randles circuit have been modelled (Fig. 10). The semi-circle curve of monomer at high frequencies is related to the parallel combination of the electric double-layer capacitance (Cdl) and the charge-transfer resistance (Rct), whereas a little band line in upward direction at low frequencies is related to the Warburg diffusion parameter.

Nyquist plot (II) for polymer showed a semi-circle curve at high frequencies while it showed a little band line in upward direction at low frequencies. To understand this system, a Randles circuit has been modelled (Fig. 11) in which the semi-circle curve of polymer at high frequencies is related to the parallel combination of the electric double-layer capacitance (Cdl) and the charge-transfer resistance (Rct) and the Warburg element has been replaced by the diffusion element ZD. The value of ZD is calculated by the following equation:

$$ZD=A\ \coth[B(j\omega)^{1/2}]/(j\omega)^{1/2} \quad (2)$$

The plot of Z *vs* $\omega^{-1/2}$ for the region of semi infinite diffusion has a slop of σ while the plot of Z *vs* ω^{-1} for the thin film has a slop of ΔC^{-1}. These values can be used to calculate the value of RF according to the following equation:

$$RF\Delta C=1/3\ (\phi/D^{1/2})^2 \quad (3)$$

$$\text{where } \sigma=1/1.41\Delta C\times(\phi/D^{1/2}) \quad (4)$$

Table 2. Heterogeneous electron transfer rate constant (K^0) and diffusion (D_0) coefficient for both macrocycles by considering one electron processes, v=100 mVs^{-1} and A=0.031 cm^2

No. of Cycles	**Fe[Me_2-DBDPy)N_6tetraoxo[18]Cl_2]Cl**		**Ni[Me_2-(DBDPy)N_6tetraoxo[18]Cl_2]**	
	$D_0\times10^{-6}$ (cm^2/s)	**$K^0\times10^{-3}$ (cm/s)**	**$D_0\times10^{-6}$ (cm^2/s)**	**$K^0\times10^{-3}$ (cm/s)**
1	1.06	1.66	7.48	7.21
2	1.64	2.07	29.41	8.79
3	2.20	2.40	44.91	10.86
4	2.84	2.73	57.69	12.31
5	3.19	2.89	68.78	13.45

The charge transfer resistance (Rct) is used to explain the overall heterogeneous transfer of electron during the polymerisation process while Warburg element (ZD) is defined as the diffusion of counter ions from the solution towards the electrode surface.

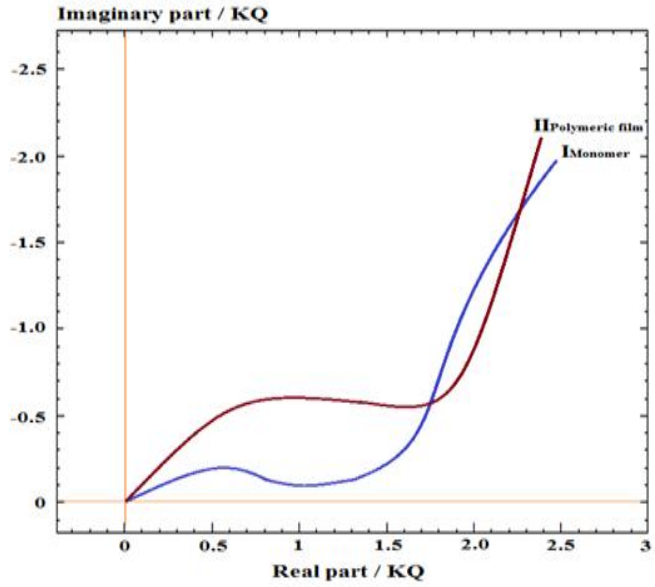

Fig. 10. (I) Nyquist plot for Ni[Me_2-(DBDPy)N_6tetraoxo[18]Cl_2] monomer (II) Nyquist plot for polymeric film of Ni[Me_2-(DBDPy)N_6tetraoxo[18]Cl_2]

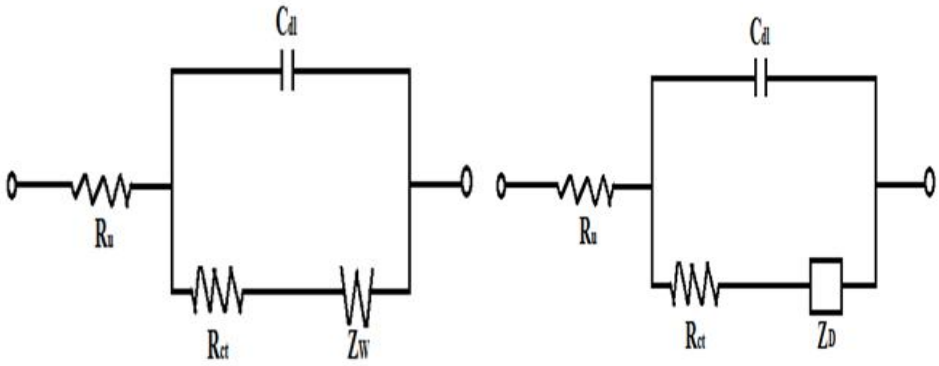

(a) **(b)**

Fig. 11. (a) Randles equivalent circuit for Ni[Me_2-(DBDPy)N_6tetraoxo[18]Cl_2] monomer; **(b)** Randles equivalent circuit for polymeric film of Ni[Me_2-(DBDPy)N_6tetraoxo[18]Cl_2]

3.5. Effect of concentration of macrocycles

Further, CVs of both macrocyclic complexes were recorded in DMSO containing 0.4×10^{-3} M of electrolyte at 200 mVs^{-1} scan rate. On increasing the concentration of electrolyte (from 0.1×10^{-3} M to 0.4×10^{-3} M), increase in the current intensity of the redox peaks is observed indicating increase in the amount of the electrodeposition on working electrode. Therefore,

the polymerisation rate is increased with increase in the concentration of the macrocyclic complexes (Fig. 12).

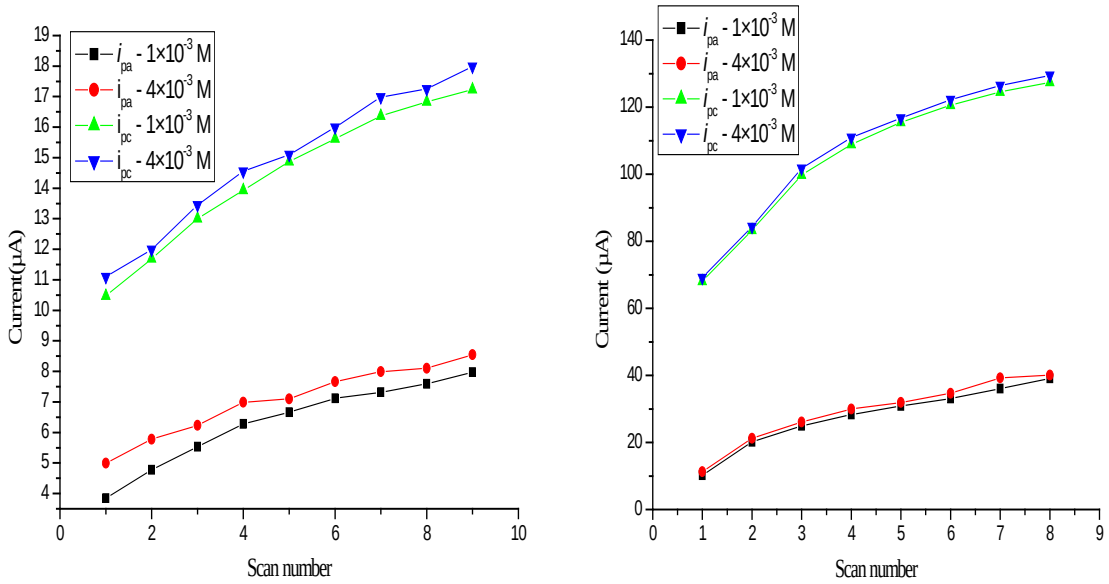

(a) **(b)**

Fig. 12. (a) Plot of current *vs* scan number of Fe[Me_2-(DBDPy)N_6tetraoxo[18]Cl_2]Cl and **(b)** Plot of current *vs* scan number of Ni[Me_2-(DBDPy)N_6tetraoxo[18]Cl_2]

4. CONCLUSION

In this communication, tetraazamacrocyclic complexes of Fe(III) and Ni(II) have been synthesized by the template method using 2,4-diaminotoluene and diethyl-2,6-pyridinecarboxylate. Cyclic voltammetric studies of the synthesized macrocycles showed the interesting results for their unusual oxidation states, on single scanning at 200 mVs^{-1} scan rate. On repeating cycles from -1.5 to +2.0 V *vs* Ag/AgCl at 200 mVs^{-1} scan rate, it resulted in the formation of polymeric film on Pt electrode which depends on the concentration of the electrolyte and the electrode surface. The CVs of both complexes showed the shifting of the oxidation peaks and reduction peaks in an anodic direction and the in the cathodic direction with the increasing in the current intensity respectively that indicates the formed polymeric film is conductive. Heterogeneous electron transfer rate constant and charge profile for both complexes also support that polymer layer take place in uniformity and is stable. UV-Visible and FT-IR spectra suggest that the macrocycles remained in the polymeric film. These surface modified electrodes are important from a number of viewpoints. Thin, homogeneous films can be deposited on the electrode surface, and the surface potentials can be controlled by varying the substitution on the ligand, the metal centre, and the ligand themselves. As the polymerisation is ligand-centred, it should be possible to prepare copolymer films coupling the appropriate macrocycles that conduct over a large potential region. It is now possible to

design rectifiers and diodes by the sequential polymerization of the appropriate macrocycles on the electrode surface. These surface modified electrodes should thencan be used in catalysis and fuel cells and could serve asin other electronic devices .

Acknowledgement

The authors are thankful to CSIR New Delhi for financial support in the past projects. Support from SAIF Panjab University Chandigarh, India is also acknowledged for analytical studies .

REFERENCES

[1] J. M. Zen, D. M. Tsai, A. S. Kumer, and V. Dharuman, Electrochem. Comm. 2 (2000) 782.
[2] J. B. Raoof, R. Ojani, and A. Kiani, J. Electroanal. Chem. 515 (2001) 45.
[3] M. Pontié, P. Cowache, L. H. Klein, V. Maurice, and F. Bédioui, J. Memb. Sci. 184 (2001) 165.
[4] J. S. Ye, Y. Wen, W. D. Zhang, L. M. Gan, G. Q. Xu, and F. S. Sheu., Electrochem Comm. 6 (2004) 66.
[5] K. Miyazaki, Y. Lee, T. Fukutsuka, and T. Abe. J. Electrochem. 80 (2012) 725.
[6] J. Ren, H. Zhang, Q. Ren, C. Xia, J. Wan, and Z. Qin, J. Electroanal. Chem. 504 (2001) 59.
[7] J. Wang, Z. Wu, J. Tang, R. Teng, and E. Wang, Electroanalysis 13 (2001) 1093.
[8] C. X. Cai, K. H. Xue, and S. M. Xu, J. Electroanal. Chem. 486 (2000) 111.
[9] J. Vatsalarani, S. Geetha, D. C. Trivedi, and P. C. Warrier, J. P. Sources. 158 (2006) 1484.
[10] F. B. Kaufman, A. H. Schroeder, V. V. Patel, and K. H. Nichols, J. Electroanal. Chem. 132 (1982) 151 .
[11] P. Daum, J. R. Lenhard, and D. R. Murray, J. Am. Chem. Soc. 102 (1980) 4649.
[12] R. J. Nowak, F. A. Schultz, M. Umana. R. Lam, and R. W. Murray, Anal. Chem. 52 (1980) 315.
[13] E. Laviron, J. Electroanal. Chem. 1 (1980) 112.
[14] B. Fisher, and R. Eisemberg, J. Am. Chem. Soc. 102 (1980) 7361 .
[15] A. J. Bard, and L. R. Faulkner, Electrochemical Methods: Fundamentals and Application, Willey, New York (2001).
[16] N Gu, and S. Dong, Electrochem. Comm. 2 (2000) 713.
[17] Y. F. Yuan, Y. Li, S. Tao, F. C. Ye, J. L. Yang, S. Y. Guo, and J. P. Tu, Electrochim Acta 54 (2009) 6617.

[18] D. V. Soldatov, P. R. Diamente, C. I. Rateliffe, and J. A. Ripmeester, Inorg. Chem. 40 (2001) 5661.
[19] A. P. Hussain, and A. Kumar, Bull. Mater. Sci. 26 (2003) 329.
[20] M. K. Motlagh, and M. Noroozifar, Turk J Chem. 28 (2004) 369.
[21] R. W. Murray, Acc. Chem. Res. 13 (1980) 135.
[22] Z. Feng, Z. Yang, J. Huang, X. Xie, and Z. Zhang, J. P. Sources 276 (2015) 162.
[23] G. A. Ragoisha, Electroanalysis 27 (2015) 855 .
[24] A. M Asiri, S. A. Khan, and I. S. E. l Hallag, J. New. Mater. Electrochem. 14 (2011) 251.
[25] E. M. Ervin, B. T. Adams, N. Snyman, C. P. Phenix, J. K. Kariuki, and B. P. Rempel, Int J. Electrochem. Sci. 9 (2014) 6043.
[26] S. Randhir, B. Ramesh, B. K. Virendra, S. Rakam, T. Kapil, and A. Shabana, Inorg. Chem. 23 (1984) 4153.
[27] R. S. Nicholson, and I. Shain, Anal. Chem. 36 (1964) 706.
[28] C. D. Ellis, L. D. Margerum, R. W. Murray, and T. J. Meyer, Inorg. Chem. 22 (1983) 1283.